Etch pit development and growth on GaAs(110)

B. Y. Han, C. Y. Cha, and J. H. Weaver

Department of Materials Science and Chemical Engineering, University of Minnesota, Minneapolis, Minnesota 55455

(Received 17 March 1997)

We used scanning tunneling microscopy to study etch pits that are formed at 650 K after exposure of GaAs(110) to Br_2 at lower temperature. Dual bias imaging reveals that 80% of the pits that are one to two rows wide correspond to pairwise removal of Ga and As from surface lattice sites. These pits tend to grow along $[1\bar{1}0]$ and have ends that are equally likely to be bounded by either Ga or As atoms. In addition, there is etching across adjacent rows. The resulting pits cross several zigzag rows and have kinked $[1\bar{1}0]$ sides and irregular ends. When these pits grow larger, they increasingly exhibit kinked $\langle 1\bar{1}2 \rangle$ boundaries and hexagonal appearances. Rebonding of As atoms at pit boundaries to exposed second-layer As atoms was observed, and an analysis of the pit boundaries indicates that there are equal numbers of As and Ga terminations. We suggest that etching along $[1\bar{1}0]$ involves removal of a Ga atom that was either a pit boundary atom or next to a rebonded As boundary atom and that such processes are equally accessible. [S0163-1829(97)04432-9]

Scanning tunneling microscopy (STM) has been used to great advantage to reveal the details of surfaces with atomic or nearly atomic resolution. Recently, several studies have emphasized the structure of terrace vacancies on III-V compound semiconductor (110) surfaces.[1,2] Calculations motivated by these observations have sought to determine the atomic and electronic structure of single-atom vacancies.[1,3] Other STM studies have observed more extended terrace defects produced by halogen etching[4,5] or inert-ion impact[6] on GaAs(110). What is missing is an investigation of the structure of pits as they evolve from a single-atom or an atom-pair vacancy to an extended structure. This evolution has similarities to what one finds in growth when adatoms form nuclei which then grow.

Here we examine the structure of small single-layer pits and their growth on GaAs(110) terraces. Using STM, we show that removal of a Ga-As pair is common in pit creation and that pit growth also favors pairwise removal. As the pits grow, they increasingly exhibit a tendency to be bounded by $\langle 1\bar{1}2 \rangle$ and $[1\bar{1}0]$ steps, though the kink density in the former is high. The atomic character of the species that bound single-layer etch pits has been determined and rebonding of pit boundary atoms with exposed second-layer atoms has been observed. The implications of these observations vis-à-vis etching mechanisms are discussed.

The experiments were performed in a vacuum chamber with a base pressure $\sim 5 \times 10^{-11}$ Torr. We exposed cleaved *p*-type GaAs(110) (Zn doped at 1×10^{18} cm^{-3}) to a molecular beam of Br_2 from a solid-state electrochemical cell, using the cell current and exposure time to control the Br_2 fluence.[4,5] The surfaces were dosed at room temperature to produce Br coverages between 0.005 and 0.5 monolayer (ML), where 1 ML$=8.84 \times 10^{14}$ cm^{-2}, the planar atomic density of GaAs(110). These starting coverages were determined by counting the Br adatoms (they appear bright in constant-current STM images[4,5]). We then annealed the sample for 20 min at 650 K, as monitored by an optical pyrometer and a Chromel-Alumel thermocouple attached to the sample holder. Images were recorded after the sample cooled to room temperature. The images presented here have

$[1\bar{1}0]$ running from lower right to upper left. Within each zigzag row, the Ga atoms are on the left and the As atoms are on the right, as determined by tunneling-voltage-dependent imaging. These images were not corrected for thermal drift.

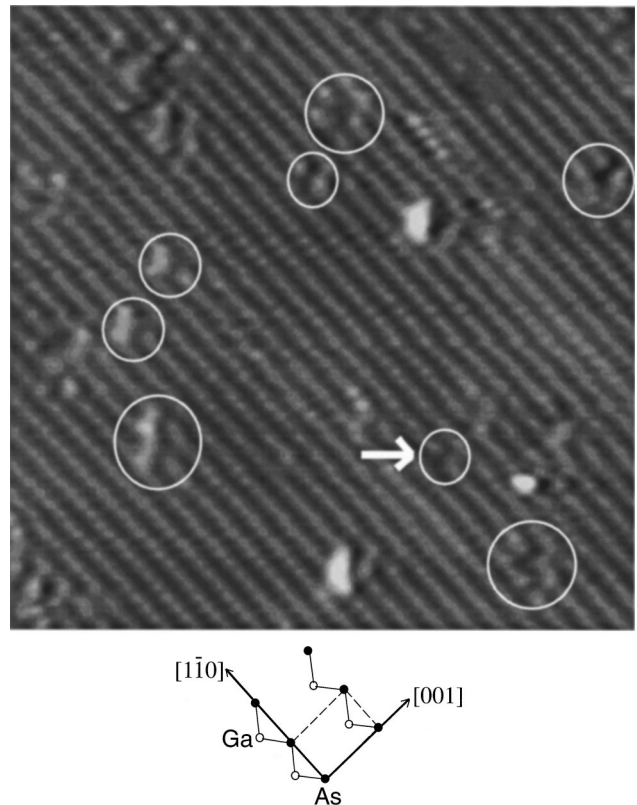Figure 1 shows the typical surface morphology obtained

FIG. 1. STM image revealing terrace pits on GaAs(110) produced by Br etching. Small single-layer deep etch pits are visible, some of which are circled. They appear as dark features that disrupt $[1\bar{1}0]$ atomic rows. Most correspond to removal of one to three Ga-As pairs along the row. The pit marked by an arrow probably reflects a Ga-As-Ga trivacancy. The surface lattice structure is shown schematically. (150×150 Å^2, As sublattice, $V_s = -2.8$ V.)
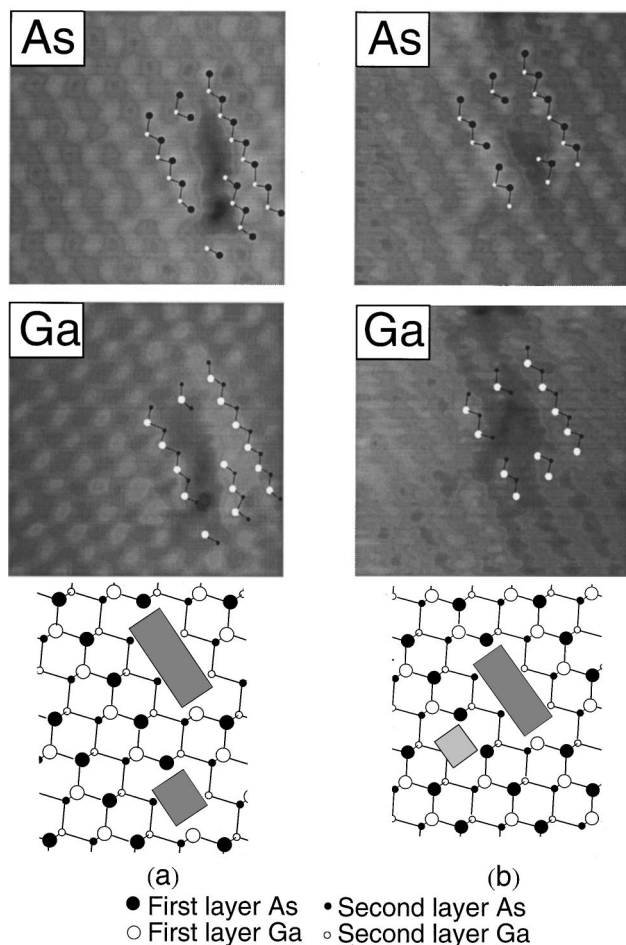
FIG. 2. Images of two etch pits that show As and Ga sublattices (50×50 Å^2). The positions of both types of atoms are indicated, with the larger dots corresponding to atoms that appear in the respective image. Both main vacancy rows reflect removal of two Ga-As pairs along [1$\bar{1}$0], bounded by an As atom at the upper end and a Ga atom at the lower end. Proposed structures are shown. (a) A single Ga-As pair vacancy appears to the left of the pit, while (b) a Ga atom vacancy is evident.

after heating when the initial Br coverage was 0.005 ML. The surface is dotted with small pits that appear as dark depressions in the zigzag rows. Most of them represent the removal of one to three Ga-As pairs. Those that are one row wide do not exceed three unit cells in length along [1$\bar{1}$0]. There are also bright spots at pit edges that reflect residual Br adatoms, as observed previously in continuous-etching studies of Br-GaAs(110) in this temperature range.[4] Hence Br adatoms that are mobile at 650 K are frozen in pit boundary sites as the sample cools to room temperature. As discussed below, Br decoration of both As- and Ga-pit boundary atoms is observed. For most of the pits in Fig. 1, the ends show different, but nonetheless well-defined, appearances when viewed with higher resolution. This is to be expected if pairwise removal of Ga-As pairs is done along [1$\bar{1}$0] since one end would be Ga terminated and the other would be As terminated. Note that heating to 650 K of GaAs(110) that was free of Br did not introduce defects of the sort identified in Fig. 1.

Insight into the identity of atoms bounding the line vacancies can be obtained through dual bias imaging. On relaxed GaAs(110), the Ga dangling bonds are empty and the As dangling bonds are full. Hence occupied-state images (negative sample bias) reveal the As sublattice, as in Fig. 1, while unoccupied-state images reveal the Ga sublattice.[7] Figure 2 shows dual-bias images for two small etch pits, labeled (a) and (b). The images were acquired simultaneously using alternating line scans in either bias so that drift would not affect the atomic registry. Identification of the species bounding the vacancy rows was done by superimposing the Ga and As sublattice images. From Ref. 1 we also note that As atoms adjacent to single Ga vacancies appear brighter in As sublattice images than do As atoms far from the defect. Likewise, Ga atoms adjacent to As vacancies appear brighter in Ga images. Here we observe similar contrast differences around etch pits, though they are of greater spatial extent. We stress that a brighter object in a STM image reflects an enhanced local density of states, not necessarily an outward atomic relaxation. This was pointed out by Kim and Chelikowsky[3] and Zhang and Zunger[3] for a single As vacancy on GaAs(110), where they deduced slight inward relaxation for Ga atoms and Ga-Ga bond formation.

Inspection of the Ga and As atomic registries in Fig. 2 reveals that the two main vacancy rows have the same structure. Both are bounded by an As atom at the upper end and a Ga atom at the lower end and both correspond to the removal of two Ga-As pairs (see the models). Inspection also shows that one Ga-As pair is missing on the row to the left of the main vacancy of pit (a). This pair vacancy is bounded by an As atom at the upper end and a Ga atom at the lower end. It could have been formed independently on the terrace or through a branching event at the main row, with subsequent diffusion away from the parent unit. Diffusion of divacancies on GaAs(110) after their creation by Ar$^+$ sputtering was discussed in Ref. 6, and the effective energy barrier was determined to be 1.3 eV. The low Br concentration used to obtain the surfaces imaged in Fig. 2 excludes significant interference of Br on vacancy diffusion, and divacancy diffusion at 650 K would have been possible. Finally, there is a single Ga vacancy in the row to the left of the main vacancy in pit (b). Such single-atom vacancies in adjacent rows are unusual, as discussed below.

Analysis of the structure of a large number of pits localized to one or two zigzag rows shows that approximately 80% were composed of pair vacancies. Hence the main growth channel for stable terrace pits involves pairwise removal of Ga and As from surface lattice sites. The desorption of Ga bromide is accompanied by the ejection of As onto the terrace. The As then diffuses until it encounters another As atom, forms volatile As$_2$ (or As$_4$), and desorbs. This conclusion is supported by considerations of larger pits, discussed below. Although concerted removal of two pairs might be facilitated by a transition state involving As-As bonding, the absence of preferred even- or odd-numbered pairs suggests that the growth increment is just one pair.

Insight into the etching channels can be gained from studies of Cl etching of GaAs, where it has been shown that desorption at 650 K involves GaCl and GaCl$_3$ in about equal amounts.[8] The similar chemistry of Br and Cl suggests that desorption GaBr and GaBr$_3$ products will be found for Br-GaAs(110). As argued elsewhere,[5] the monohalide channel (low Br concentration, high desorption barrier channel) is
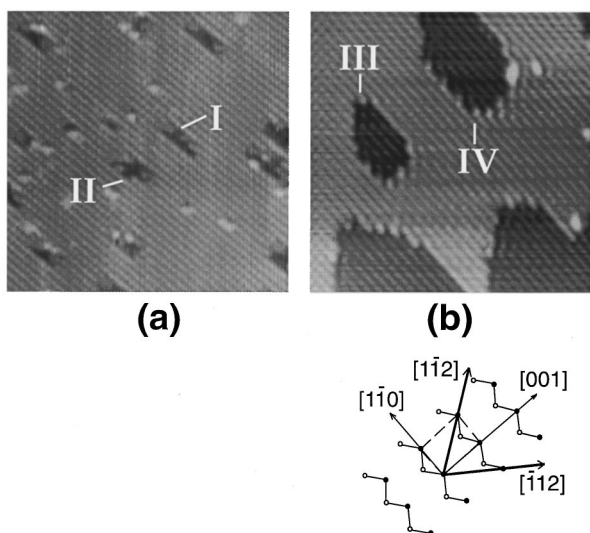
FIG. 3. Representative As sublattice images of GaAs(110) etched at 650 K for initial Br coverages of (a) 0.015 ML and (b) 0.2 ML. The pits are larger than in Fig. 1 because of growth along $[1\bar{1}0]$ and kink creation/propagation on adjacent rows. Arrows I and II point to kink sites on Ga and As $[1\bar{1}0]$. In (b), large, single-layer pits III and IV are bounded by segments of $[1\bar{1}0]$ and kinked $\{1\bar{1}2\}$ steps. Some As $[1\bar{1}0]$ steps show $4\times$ periodicity. Misalignment between the axes of the image and the model is caused by thermal drift. [(a) 250×250 Å^2 and (b) 200×200 Å^2.]

associated with growth of established pits along the row direction, while the trihalide channel (high Br concentration, low desorption barrier) facilitates terrace pit initiation and kink formation in adjacent zigzag rows. In addition, desorption of As$_2$ and As$_4$ has been observed at 650 K.[8] As$_4$ is the more volatile species, but it is unlikely to form under our conditions of low etchant concentration. Supporting evidence for the release of As onto the terrace associated with Ga desorption comes from observations of small amounts of As on surfaces annealed at 650 K for 20 min. These features were located between As rows, seemingly coordinated with Ga. They appeared to be weakly bound to the surface since tip-induced motion was observed under typical tunneling conditions ($V_s = 1.5-3$ V, $I_s = 0.15-0.2$ nA).

While most small pits consist of pair vacancies, there are some that reflect the absence of an odd number of atoms. An example is the single Ga vacancy near pit (b) in Fig. 2. Since isolated Ga vacancies are not observed on our cleaved p-type GaAs(110) samples or on those that are heated to 650 K without Br, we conclude that it was created by Br etching. The rarity of single Ga vacancies is consistent with studies of point defects on cleaved p-type GaAs.[1] The arrow in Fig. 1 points to another odd-length vacancy, corresponding to a pit that is 8 Å long and one row wide. The bright and symmetric appearance of its ends in the As sublattice image suggest that it is a Ga-As-Ga trivacancy. One way that an odd-number vacancy could be produced would involve capture of a mobile As adatom by an even-numbered vacancy.

Figure 3 shows representative STM images (occupied-state, As sublattice images) that were obtained after heating samples with initial Br coverages of 0.015 and 0.2 ML. A comparison to Fig. 1 reveals growth along the zigzag rows and across them. Most pits of Fig. 3(a) extend over one to

three rows and they are two to eight unit cells long, corresponding to the removal of between two and twenty Ga-As pairs. All pits longer than three unit cells along $[1\bar{1}0]$ cross at least two rows. Kinks are apparent on Ga- and As-edged $[1\bar{1}0]$ steps. For example, the arrow labeled I identifies a kink in the Ga $[1\bar{1}0]$ row that reflects two missing Ga-As units. The arrow labeled II points to a kink in an As $[1\bar{1}0]$ row that is three units in length, adjacent to a parent that is two rows wide. Analysis of hundreds of pits revealed that 60% have kinks on both sides. Of the remaining 40%, kink creation is favored on Ga $[1\bar{1}0]$ by a factor of about 2, giving a bias in favor of Ga $[1\bar{1}0]$ kinks of 54:46. The lack of preferred kinking on one side or the other is consistent with a previous study of continuous thermal etching in this temperature range, although they investigated pits that extended over six or more rows because of their larger Br fluence.[4]

Kink creation can occur at either end of a pit or at a midpoint along the pit. Once formed, the kink can grow along $[1\bar{1}0]$ analogously as the parent. Extended growth after creation tends to align the ends of parent and daughter rows and makes it impossible to determine where formation occurred. For pits where the kinks were only a few units in length and could be related to an end or a center position, the center positions outnumbered the ends by roughly a factor of 3.[9] For the daughter rows, about 80% correspond to the removal of Ga-As pairs. This indicates a similar pairwise removal mechanism, as in the initial etching stages.

Figure 3(b) shows an occupied-state image of GaAs(110) etched at 650 K with 0.2-ML initial Br coverage. Large, single-layer etch pits were formed, typically reflecting the removal of several hundred Ga-As pairs. These pits exhibit hexagonal shapes established by kinked segments of $[1\bar{1}0]$ and $\langle 1\bar{1}2 \rangle$ steps. (See the schematic for some principal surface directions. Misalignment between the axes in the images and the model is caused by thermal drift.) A few residual Br atoms decorate the pit edges. Visual inspection of the $\langle 1\bar{1}2 \rangle$ steps reveals termination by both As and Ga atoms, as confirmed by dual-bias imaging (see Fig. 4). This suggests similar etching behavior at rows terminated with either Ga or As. By this stage in pit growth, the step lengths along $\langle 1\bar{1}2 \rangle$ are increasing and the pit shapes are indicative of step energies. This tendency is analogous to that observed in growth where the shape of an island composed of a few atoms is often ill defined, but it exhibits low-energy facets as it grows. The $\langle 1\bar{1}2 \rangle$ steps represent a more favorable pit boundary than other steps such as $[001]$, as confirmed by considerations based on local charge balance requirements (electron counting model).[10] Some As $[1\bar{1}0]$ steps created by etching show bright spots that exhibit $4\times$ periodicity (or, less frequently, $3\times$ periodicity), as in pit IV. A $2\times$ structure observed on As $[1\bar{1}0]$ boundaries of double-layer etch pits has been related to As trimer-like reconstructions.[4] The exact origin for single height steps, however, is not known.

Figure 4 shows dual-bias images obtained after exposing to 0.05 ML [pit (a)] and 0.5 ML of Br [pit (b)], with subsequent heating to 650 K. These results make it possible to deduce the structure of extended pits. There is a bright spot on the upper left edge of pit (a) that is evident in both biases on a $[1\bar{1}2]$ step. This reflects a residual Br adatom because there are bonding and antibonding states of Br-Ga or Br-As on GaAs(110) that are partially accessible
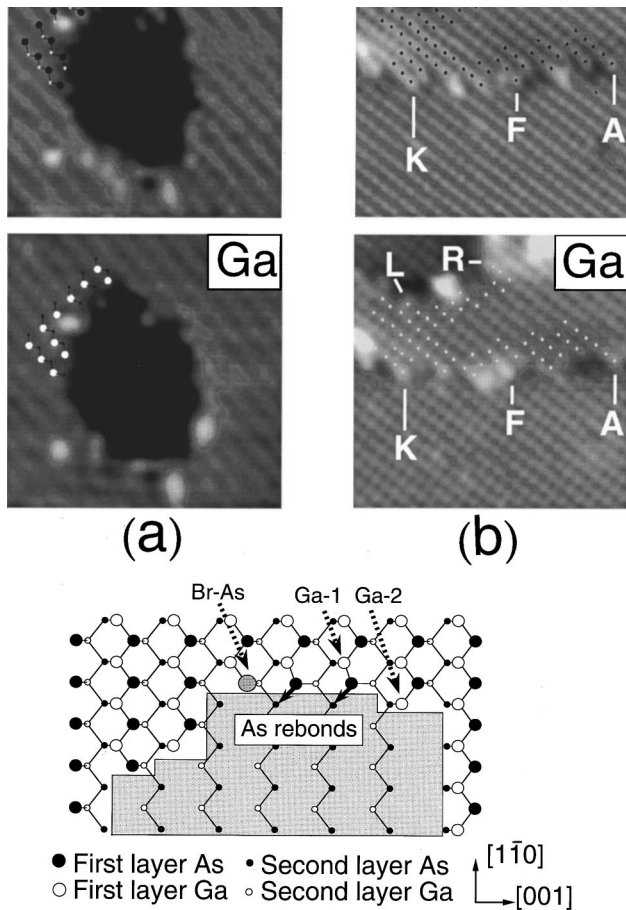
FIG. 4. Dual-bias images showing bounding species of a large pit and a residual top-layer structure created by etching from initial Br coverages of 0.05 and 0.5 ML (annealing temperature 650 K). In the latter, approximately 80% of the top layer has been removed. The apparent positions of some As and Ga atoms are marked by black and white dots in their respective sublattices. The schematic represents the structure of the upper left edge of pit (a). Arsenic atoms at the pit boundary are depicted as rebonded with second-layer As atoms. The text discusses etching of Ga atoms from sites like those labeled Ga-1 and Ga-2. In (b), the row ends are represented by the letters $A-R$, though only a few of the letters are given to avoid clutter. The features terminating the rows in (b) are Ga atoms (rows A, C, G, L, and Q) and As atoms (B, E, K, M, P, and R). Residual Br is bonded to Ga at F, H, and O and to As at I. Row D appears to be terminated with an adsorbed As_2 structure. [(a) 75×75 Å^2 and (b) 115×115 Å^2.]

under our tunneling conditions ($V_s = 1.9 - 3.2$ V).[4] From the As and Ga sublattice images, this Br adatom is atop an As atom at the pit boundary. This site is labeled Br-As in the model beneath the image. The three rows to the right are, respectively, As, As, and Ga terminated. The registries of the two As atoms appear inclined to the left relative to the neighboring zigzag rows. We associate this distortion with As rebonding to second-layer As at the step, as depicted in the model. The two neighboring rows to the left of the Br feature are Ga and As terminated, respectively. While we find evidence for As rebonding, the experimental results are inconclusive regarding Ga rebonding, though such a process at a step is possible. Gallium dimerization has been reported at Ga-terminated GaAs(100) (Refs. 12 and 13) and Ga-Ga

bonding has been deduced at single As vacancies on GaAs(110).[3]

The image of Fig. 4(b) was obtained after removal of $\sim 80\%$ of the first layer (initial Br coverage 0.5 ML, etch yield 1.6, consistent with Brake et al.[5]). The remnant of the first layer crosses the image from the middle left to the right corner with row ends labeled $A-R$. To avoid clutter, we have labeled only a few of the rows. The termination of most rows can be identified by comparing registries in As and Ga sublattice images. Again, As atoms tend to rebond with second-layer As neighbors (terminations B, E, J, K, and R). The bright spot between rows F and G in the As sublattice image reflects a feature atop a Ga atom in row F. This is confirmed in the Ga sublattice image where there is a bright spot in row F. A comparison of its position with neighboring rows in both sublattices establishes that row F is terminated by an As atom with a Br atom atop its Ga neighbor in the same row. This points to favorable bonding of Br to Ga along As-terminated zigzag rows. Row D shows a bright spot in the As sublattice, which coincides with a dark spot in the Ga sublattice. We assign this to an As atom atop another As at the row end.

Etch pit growth patterns are determined by desorption barriers for volatile species at different surface positions, subject to local Br concentrations. Simple considerations suggest that etching should be favored along $[1\bar{1}0]$, where the Ga or As atoms are nominally twofold coordinated. Atoms forming $[1\bar{1}0]$ steps conserve all three bonds and are more tightly bound than the twofold coordinated atoms, but are less well bound than atoms on defect-free terraces. The statistics for kink creation on Ga $[1\bar{1}0]$ and As $[1\bar{1}0]$ suggest that such processes on the two steps have about the same overall energy barrier. For a medium sized pit such as III in Fig. 3(b), which extends over six rows, at least five high-activation-energy kink events must have occurred after pit initiation. Elongation along $[1\bar{1}0]$ would have been the dominant material removal channel, accounting for roughly 70 events. Unfortunately, it is not possible to deduce the energy difference between kinking and $[1\bar{1}0]$ elongation since different etching channels prevail in the two cases ($GaBr_3$ desorption in the former and GaBr desorption in the latter).

We can also compare etching along $[1\bar{1}0]$ for Ga and As bounding species. In the schematic of Fig. 4, Ga-1 marks a Ga atom adjacent to an As bounding atom; Ga-2 marks a Ga atom that serves that function. Similar configurations can be seen in Fig. 3(b). This frequently observed alternation from row to row strongly suggests that etching is equally likely at Ga- and As-terminated vacancy rows. This is intriguing, as one might expect from bond counting that a Ga atom adjacent to an As termination might be more strongly bound than a Ga atom that is itself the termination (the former has three backbonds and the latter has only two). However, as was shown in Figs. 3 and 4, the As atoms at pit boundaries rebond with their second-layer neighbors. This probably weakens the bond between the rebonded As atom and its Ga neighbor and facilitates the removal of the latter as GaBr. The validity of this intuitive picture remains to be verified. Model calculations would need to consider the transition states associated with Br atom(s) at relevant positions around the pit and the barriers for GaBr desorption.

When considering the details of pit formation, it is important to recognize the tendency of Br adatoms on GaAs(110) to form islands.[4,11] Once formed, Br diffusion from centrally located sites is impeded by neighboring Br atoms by site blocking. Accordingly, the concentration of Br remains high and such areas are favored for pit formation and expansion. The shape distribution of etch pits obtained through the expose/anneal cycle investigated here should then be quite different from that produced by continuous etching at elevated temperature with fixed (low) halogen fluxes. In our process, the initial concentration is selected and islands are formed at room temperature. Upon heating, the concentration diminishes as desorption is activated. In continuous etching, the steady-state surface concentration reflects the balance between dissociative Br adsorption and etching at elevated temperature.

The pit boundaries are likely to be dynamic at 650 K, with atom rearrangement that would affect the local structure.[5] In our experiments, however, we found no evidence that heating to 650 K would induce atom evaporation from pit edges that would change the relative amount of Ga and As. Indeed, analysis of the sort described above indicates that the pit boundaries and steps are made up of equal numbers of Ga and As atoms. This satisfies global electron counting and ensures charge neutrality.

In summary, Br etching of GaAs(110) at 650 K has been shown to involve the formation of single-layer deep etch pits that preferentially grow via pairwise removal of Ga-As pairs along [1$\bar{1}$0]. Pairwise removal is also associated with kink creation and propagation at [1$\bar{1}$0] steps. Etching along [1$\bar{1}$0] produces both As and Ga termination, with equal population. The similar etching behavior along [1$\bar{1}$0] undoubtedly reflects rebonding of As boundary atoms with second-layer As atoms and possibly rebonding of Ga as well. Such effects influence the desorption barriers for GaBr.

[1] G. Lengel, R. Wilkins, G. Brown, M. Weimer, J. Gryko, and R. E. Allen, Phys. Rev. Lett. **72**, 836 (1994); G. Lengel, R. Wilkins, G. Brown, and M. Weimer, J. Vac. Sci. Technol. B **11**, 1472 (1993).

[2] Ph. Ebert, K. Urban, and M. G. Lagally, Phys. Rev. Lett. **72**, 840 (1994).

[3] H. Kim and J. R. Chelikowsky, Phys. Rev. Lett. **77**, 1063 (1996); S. B. Zhang and A. Zunger, *ibid.* **77**, 119 (1996).

[4] J. C. Patrin and J. H. Weaver, Phys. Rev. B **48**, 17 913 (1993).

[5] C. Y. Cha and J. H. Weaver, J. Vac. Sci. Technol. B **14**, 3559 (1996); C. Y. Cha, J. Brake, B. Y. Han, D. W. Owens, and J. H. Weaver, *ibid.* **15**, 605 (1997); J. Brake, C. Y. Cha, B. Y. Han, D. W. Owens, and J. H. Weaver, *ibid.* **15**, 670 (1997).

[6] X.-S. Wang, R. J. Pechman, and J. H. Weaver, Appl. Phys. Lett. **65**, 2818 (1994); R. J. Pechman, X.-S. Wang, and J. H. Weaver, Phys. Rev. B **51**, 10 929 (1995).

[7] R. M. Feenstra, J. A. Stroscio, J. Tersoff, and A. P. Fein, Phys. Rev. Lett. **58**, 1192 (1987).

[8] C. Su, H.-Q. Hou, G. H. Lee, Z.-G. Dai, W. Luo, M. F. Vernon, and B. E. Bent, J. Vac. Sci. Technol. B **11**, 1222 (1993), investigated steady-state etching of GaAs(100) as a function of temperature with a Cl_2 flux of 3 ML/s.

[9] Midpoint branching along a vacancy row for GaAs(110) is quite different from what occurs on Si(100) where chains of missing dimers develop along the dimer row direction. A quantitative analysis of the images for etching Si(100) indicates that endpoint branching is favored over midpoint branching by an energy of ~0.08 eV. See J. R. Sánchez, C. M. Aldao, and J. H. Weaver, J. Vac. Sci. Technol. B **13**, 2230 (1995).

[10] J. M. McCoy and J. P. LaFemina, Phys. Rev. B **54**, 14 511 (1996).

[11] J. L. Corkill and J. R. Chelikowsky, Phys. Rev. B **53**, 12 605 (1996).

[12] T. Hashizume, Q. K. Xue, J. Zhou, A. Ichimiya, and T. Sakurai, Phys. Rev. Lett. **73**, 2208 (1994); T. Hashizume, Q. K. Xue, A. Ichimiya, and T. Sakurai, Phys. Rev. B **51**, 4200 (1995).

[13] J. Behrend, M. Wassermeier, L. Daweritz, and K. H. Ploog, Surf. Sci. **342**, 63 (1995).